

Mean JHK Magnitudes of Fundamental-Mode Cepheids from Single-Epoch Observations

I. Soszyński^{1,2}, W. Gieren¹, G. Pietrzynski^{1,2}

soszynsk@astrouw.edu.pl

wgieren@astro-udec.cl

pietrzyn@hubble.cfm.udec.cl

ABSTRACT

We present an empirical method for converting single-point near-infrared J , H , and K measurements of fundamental-mode Cepheids to mean magnitudes, using complete light curves in V or I bands. The algorithm is based on the template light curves in the near-infrared bandpasses. The mean uncertainty of the method is estimated to about 0.03 mag, which is smaller than the uncertainties obtained in other approaches to the problem in the literature.

Subject headings: stars: Cepheids - stars: oscillations - infrared: stars

1. Introduction

In recent years great effort has been devoted to calibrating the near-infrared (NIR) period-luminosity (PL) relationship of Cepheids. There are numerous advantages of observing Cepheids in J , H , or K bands compared to optical observations. First, the dust extinction is an order of magnitude lower than in the visual bandpasses. Second, the spread around the mean PL relation is smaller. Third, metallicity effects on the PL relation are expected to decrease in amplitude with increasing wavelength.

The largest difficulty in achieving good-quality NIR PL diagrams for Cepheids is the necessity of obtaining well-covered light curves to compute the mean magnitudes. However, the techniques of observations in NIR passbands are more time-consuming, the sizes of NIR detectors are in general significantly smaller than the optical detectors, and NIR imagers are not as widely available on telescopes and are frequently “bright time” instruments. Therefore, usually only one or two random-phase observations of Cepheids in the J , H , or K bands are available. It is then necessary to recover the mean magnitudes of the Cepheids from few-epoch data. While such corrections to derive the

¹Universidad de Concepción, Departamento de Física, Casilla 160-C, Concepción, Chile

²Warsaw University Observatory, Al. Ujazdowskie 4, 00-478 Warszawa, Poland

mean magnitudes are usually not the dominant remaining errors for the distance determination of galaxies from Cepheids, it is still clearly desirable to keep these errors as low as possible.

One solution that can substitute for deriving mean magnitudes from complete light curves is an estimation of the average brightness by template-fitting procedures. A number of methods have been applied to reconstruct the light curves of Cepheids in various passbands.

Historically, the first method of recovering mean JHK magnitudes from single-phase observations was described by Welch et al. (1984). They suggested choosing 1 of 23 Galactic Cepheid light curves (with a period similar to the considered variable), scaling its amplitude, and using it as a template light curve to estimate the mean magnitude.

Freedman (1988) derived the V and I -band light curves of Cepheids in IC 1613 by scaling the amplitudes and shifting phases of the B -band light curves. The adopted amplitude ratios and phase lags between photometric bandpasses were calculated using 20 classical Galactic Cepheids. Freedman's solution assumed that the shapes of the light curves in the various bandpasses are the same, differing only in amplitude and phase. This assumption works well in transformations between light curves in the optical part of the spectrum, but is useless when transforming the optical to NIR light curves, because the shapes of the light curves are completely different.

A series of V and I -band template light curves were constructed by Stetson (1996). He used more than 100 Galactic and LMC Cepheids to derive mean Fourier coefficients of their light curves for a range of periods. The templates were then used to recover mean magnitudes of Cepheids from a sparsely data observed by the *Hubble Space Telescope* (Gibson et al. 2000).

Another solution to this problem was introduced by Labhardt, Sandage & Tamman (1997), who determined the correction curves to transfer V to B , R , and I -band light curves of Cepheids. They used a rather small sample (six) of Galactic Cepheids. The advantage of this method is that it does not assume fixed shapes of the template light curves.

Ngeow et al. (2003) used statistical relations between Fourier amplitudes and phases of V and I -band light curves (so-called Fourier interrelations) to reconstruct the latter. This method works properly when accurate measurements of the Fourier coefficients to the fourth order are available; i.e., when good quality well-covered V -band light curves are available.

Recently, Nikolaev et al. (2004) converted random-phase JHK measurements to mean magnitudes, computing the correction functions for each bandpass. They used more than 2000 Cepheids from the Large Magellanic Cloud (LMC) to derive the differences between the observed magnitudes of individual variables and those derived from fitted PL relations. The obtained residuals were then fitted by a function depending on the V phase. The weakest point of this method is that it does not take into account the different amplitudes of individual Cepheids. Nikolaev et al. (2004) estimated the errors of their method as 0.05 mag. Similar uncertainties for the estimation of mean JHK magnitudes were obtained by the authors of the other algorithms described above.

In this paper, we develop a technique of deriving mean NIR magnitudes of fundamental-mode

Cepheids using one random-phase measurement in J , H , or K bands and the complete light curves observed in V or I bands. Our method is based on the template light curves in the J , H , and K bands obtained from 61 fundamental-mode Cepheids from the Milky Way and the LMC. The amplitudes of our templates depend on the amplitudes in the visual passbands (V or I bandpasses) and on the periods of the stars. The phase lags between visual and NIR light curves are constant in our algorithm.

Our paper is organized as follows. In Section 2 we present the development of the J , H , and K template light curves, in Section 3 we describe the practical application of the method of deriving mean magnitudes from single-epoch points, in Section 4 the error analysis is presented, and Section 5 contains a summary and conclusions.

2. Template development

We started our analysis by selecting the most numerous possible sample of fundamental-mode Cepheids with well-covered light curves in the NIR and visual passbands. We used J , H , and K -band observations from two sources: Laney & Stobie (1992) for Galactic Cepheids and Persson et.al (2004) for the LMC Cepheids. The former provide photometry in the Carter system, while the latter use JHK_s magnitudes in the LCO system. Since in the ongoing Araucaria Project (Gieren et al. 2001) we calibrated our NIR observations of Cepheids in several nearby galaxies onto the UKIRT system, we used Carpenter's (2001) transformation equations between NIR photometric systems to transform the photometry from both sources to this system. However, the photometric system used in our analysis is not a crucial point, because the transformation formulae between the systems depend only weakly on color, so they do not significantly influence the shapes and amplitudes of the light curves.

For the selected Cepheids, we tried to find as many Johnson V and Cousin I -band observations in the literature as possible, to obtain complete light curves in these bands. Ultimately, our list included 30 fundamental-mode Cepheids from the Galaxy and 31 stars from the LMC. Tab. 1 contains the full list of objects. The last column presents information about the sources of the adopted data.

We collected V and I photometric data covering a time span of several to more than 20 years. We used these data to correct the pulsational periods of our sample Cepheids. In most cases the periods were measured with an accuracy better than $5 \times 10^{-5}P$. We provide the improved periods in Tab. 1. Precisely determined periods are necessary to derive correct phase shifts between optical and NIR points.

A seventh-order Fourier series was then fitted to each V and I light curve. The J , H , and K light curves were fitted by a fifth-order Fourier expansion. In this way, we obtained the basic parameters of the selected Cepheids: magnitudes, amplitudes, and time of the maximum and minimum brightness. In the next part of this section, we present the development of the JHK

templates relative to V -band light curves. The analysis of the NIR photometry relative to the I bandpass was performed in the same manner.

In Fig. 1 we present the phase lags of JHK light curves relative to the V -band data plotted against the $\log P$. Note that the difference of phases depends very weakly, if at all, on period. In the further analysis, we assumed that the phase lag between visual and NIR light curves does not depend on the periods of the Cepheids.

Similarly, we tested a relationship between the amplitude ratios and the periods. Fig. 2 presents A_λ/A_V versus $\log P$ diagrams ($\lambda = \{J, H, K\}$). In each of the three panels, it is possible to notice that the amplitude ratios are smaller for the short-period Cepheids and larger for long-period Cepheids. In our algorithm, we approximated the amplitude ratios by constant values different for shorter and longer periods of variability. We adopted the same amplitude ratios for Galactic and LMC Cepheids, but a different period dividing up the values. For the Galactic Cepheids, we adopted $\log P = 1.3$, while for the LMC we used $\log P = 1.1$. The difference in the amplitude ratios between Galactic and LMC Cepheids agrees with the results of Paczyński & Pindor (2000), who found statistically significant differences in the amplitudes between Galactic, LMC, and SMC Cepheids in the period range $1.1 < \log P < 1.4$.

Tab. 2 contains the adopted amplitude ratios for the shorter and longer period Cepheids. Although the drop of the amplitude ratios around $\log P \approx 1.3$ ($\log P \approx 1.1$ for the LMC Cepheids) is clearly visible in Fig. 2, the difference between shorter and longer period stars is comparable to the scatter of the points. Therefore, the sudden adopted change of the amplitude ratio does not have a significant influence on the final results. One can determine and adopt another relationship of the amplitude ratios and periods. In particular, we call attention to Cepheids with periods longer than 100 days, for which the ratios of the NIR and V amplitudes are significantly larger than for other Cepheids.

In the next stage of our procedure, we prepared the normalized JHK light curves. For each observing point we calculated the phase from maximum brightness in the V bandpass; i.e.,

$$\phi = \text{mod} \left(\frac{JD^\lambda - JD_{max}^V}{P} \right) \quad (1)$$

The magnitudes were transformed in such a way that the mean magnitude of every light curve was 0 and the amplitude was equal to 1; e.g., for K -band points:

$$T = (K - \langle K \rangle)/A(K) \quad (2)$$

where $A(K) = K_{max} - K_{min}$ is the amplitude of variability and $\langle K \rangle$ is a magnitude-averaged mean brightness.

All points of all light curves normalized in that manner are plotted together in Fig. 3. The left panels show J , H , and K data of the Galactic Cepheids, while the right panels contain LMC data. Note that the normalized light curves are very homogeneous. The scatter of the points for

the LMC Cepheids is larger than that obtained for the Galactic variables, which is an effect of larger measurement errors for the fainter LMC objects, but the shapes of the light curves in both environments are very similar. This feature can be used to construct NIR template Cepheid light curves.

The last step of our analysis was an approximation of the co-added (Galactic and LMC Cepheids) normalized light curves using a Fourier series of seventh order:

$$T(\phi) = \sum_{i=1}^7 [A_i \cos(2\pi\phi + \Phi_i)] \quad (3)$$

which were done separately for J , H and K data. The Fourier coefficients, A_i and Φ_i , are presented in Tab. 3.

3. Application of the method

Before starting to derive the mean $\langle J \rangle$, $\langle H \rangle$, or $\langle K \rangle$ magnitudes of a Cepheid, one should make sure that its period is sufficiently well determined to accurately calculate the ephemeris phase at the individual NIR observations. If a precise period and well-covered light curves in V or I of a fundamental-mode Cepheid are available, one can easily estimate its $\langle J \rangle$, $\langle H \rangle$, and $\langle K \rangle$ using a single-epoch measurement in these filters. The procedure is as follows.

1. Determine amplitudes in the visual passbands $A(V)$ or $A(I)$, defined as the differences between the maximum and the minimum magnitude. Then using the amplitude ratios listed in Tab. 2, estimate the amplitude in the appropriate NIR bands.
2. Measure the epochs of maximum brightness in V or I bandpasses and calculate the appropriate phases of the NIR measurement points (equation 1).
3. Calculate the value of the template light curve $T(\phi)$ for a given phase using equation 3 and the Fourier coefficients listed in Tab. 3. The final estimation of the mean magnitudes can be obtained from the formulae

$$\begin{aligned} \langle J \rangle &= J - A(J) \times T_J(\phi) \\ \langle H \rangle &= H - A(H) \times T_H(\phi) \\ \langle K \rangle &= K - A(K) \times T_K(\phi) \end{aligned} \quad (4)$$

In that manner we can estimate the magnitude-averaged luminosity of the Cepheids. However, in many cases the intensity-averaged mean magnitudes are needed. To derive NIR intensity means expressed in magnitudes ($\langle J \rangle_i$, $\langle H \rangle_i$, and $\langle K \rangle_i$), we suggest using corrections to the magnitude-averaged magnitudes. For each fundamental-mode Cepheid in our sample, we determined mean

NIR magnitudes using both methods. Fig. 4 shows the differences between both mean magnitudes versus the amplitude in an appropriate bandpass. Note that the difference between magnitude-averaged and intensity-averaged mean magnitudes clearly depends on the amplitude of variability, but stays small (< 0.015 mag) even for the largest amplitudes. It is possible to easily derive intensity-averaged mean magnitudes using the following relationships, approximated by quadratic functions:

$$\begin{aligned}\langle J \rangle - \langle J \rangle_i &= 0.0072A(J) + 0.0313(A(J))^2 \\ \langle H \rangle - \langle H \rangle_i &= 0.0056A(H) + 0.0329(A(H))^2 \\ \langle K \rangle - \langle K \rangle_i &= 0.0037A(K) + 0.0366(A(K))^2\end{aligned}\quad (5)$$

To test our algorithm on independent data, we applied it to single-epoch JHK measurements of Cepheids in the LMC from the Two Micron All Sky Survey (2MASS) Point Source Catalog. We used the OGLE-II catalog of Cepheids in the LMC (Udalski et al. 1999) to select fundamental-mode Cepheids, and match them with sources from the 2MASS catalog. We found 458 counterparts closer than $2''$ from the position of the OGLE Cepheids. We then plotted single-epoch JHK measurements in the PL diagram and removed from our sample stars that were evidently blended in the 2MASS database. We recognized as blends objects deviating from the mean PL relationship by more than 3σ . This seems a reasonable assumption, given the crowding conditions in the LMC and the relatively large $2''$ size of the pixels of the 2MASS data, which increases the number of unresolved Cepheids compared to the optical OGLE images, which were taken at pixel scales of $0.4''$ per pixel. Indeed, all the objects suspected of being blends in the 2MASS data are Cepheids lying close to the respective ridge lines in the optical BVI PL relations. We selected a total of 422 stars. The 2MASS photometry was transformed to the UKIRT system using Carpenter’s (2001) formulae.

To derive mean JHK magnitudes, we utilized the well-sampled OGLE I -band light curves of the Cepheids. For each object, we performed the procedure described above. The results are presented in Fig. 5. The top panel shows the original single-epoch measurements, while the bottom panel presents the mean magnitudes derived from the application of our algorithm. The improvement is clearly visible to the naked eye, especially for longer period variables where measurement errors are smaller. For Cepheids with $P > 10$ days the scatter of the points after correction is reduced to half.

4. Error analysis

An estimation of the errors of the derived mean magnitudes was conducted using the same Galactic and LMC Cepheids that served to calibrate the method. We used each single point of each J , H , and K light curve to estimate the mean magnitudes, and we compared these values with the phase-averaged magnitudes obtained from an integration of the complete light curves. For each

Cepheid, we calculated the σ of the scatter of the estimated mean values around the “real” mean magnitudes. The data we obtained are presented in Tab. 4.

Obviously, the errors determined in this way are not the intrinsic errors of our algorithm. The scatter of derived mean magnitudes also has other causes: photometric measurement errors of the points that were used to estimate the mean luminosity, uncertainty of the settled phases and amplitudes, and errors of the mean magnitudes used to compare our results. The standard errors in the individual measurements of the Galactic Cepheids were estimated to be about 0.01 mag (Laney & Stobie 1992). The typical uncertainty of the LMC data is between 0.02 and 0.05 mag Persson et.al (2004). Formal errors of amplitudes and mean magnitudes are equal to 0.01–0.03 mag. The uncertainty of the phase lags between optical and NIR light curves is a function of the period errors and time span between observations in both bandpasses. In some cases the phase errors are as large as 0.05. The quality of the final mean magnitudes strongly depends on the accuracy of the ephemeris phase determination. We checked that a 0.05 inaccuracy in the phase lags increases the scatter of the derived mean magnitudes by a factor 2.

As one can see in Tab. 4, the typical variance of the estimated mean magnitude is about 0.03 mag for Galactic Cepheids (median values 0.035, 0.029 and 0.027 mag for J , H and K bands, respectively) and 0.05 mag for the LMC variables (0.056, 0.046, and 0.048 mag for J , H and K). The larger scatter for the LMC Cepheids is probably an effect of larger errors of individual measurements, compared to the Galactic Cepheid measurements of Laney & Stobie (1992), and the added effect of crowding on the measurements. For several Cepheids in both galaxies, the scatter is significantly larger than typical. We found that most of these cases are caused by atypical amplitude ratios (e.g., for Cepheids with $P > 100$ days) or phases lags between the V and NIR light curves. In this are also a number of Cepheids with bumps in their light curves.

Finally, the intrinsic error of our method of deriving mean NIR magnitudes of fundamental-mode Cepheids can be conservatively estimated to be 0.03 mag. The errors can be larger when the light curves are bumpy or have atypical shapes, but the accuracy can be better than 0.03 mag for Cepheids with typical light curves, when the phase lags are determined with high precision. Obviously, the larger the number of isolated JHK measurements, the better the accuracy of the final mean magnitude, because it can be averaged from several independent values.

5. Summary

The application of template light curves is the most accurate method of estimating mean NIR magnitudes of Cepheid variables when the observed data have poor phase coverage. We show that it is possible to reconstruct the NIR light curves if basic parameters of the optical light curves are available. The advantage of our method is that there is no need to determine the Fourier coefficients for the template light curves, which for sparsely sampled light curves cannot be measured accurately.

Obviously, the NIR templates can also be used without knowledge of the V or I light curves.

If several points in J , H , or K bands are available and the period of the given fundamental-mode Cepheid is known, one can fit the proper amplitudes and phases using, for instance, the least-squares method. It is an alternative method of converting the J , H , and K magnitudes to $\langle J \rangle$, $\langle H \rangle$, and $\langle K \rangle$.

Acknowledgments

W.G. and G.P. gratefully acknowledge financial support for this work from the Chilean Center for Astrophysics FONDAP 15010001. Support from the Polish KBN grant 2P03D02123 and BST grant to Warsaw University Observatory is also acknowledged.

This publication makes use of data products from the Two Micron All Sky Survey, which is a joint project of the University of Massachusetts and the Infrared Processing and Analysis Center, California Institute of Technology, funded by the National Aeronautics and Space Administration and the National Science Foundation.

REFERENCES

Barnes, T.G., Fernley, J.A., Frueh, M.L., Navas, J.G., Moffett, T.J., and Skillen, I. 1997, PASP, 109, 64

Berdnikov, L.N., Dambis, A.K., Vozyakova, O.V. 2000, Astron. Astrophys. Suppl. Ser., 143, 211

Berdnikov, L.N., & Turner, D.G. 2001, ApJS, 137, 209

Bersier, D. 2002, ApJS, 140, 465

Carpenter, J.M. 2001, AJ, 121, 2851

Coulson, I.M., Caldwell, J.A.R., & Gieren, W.P. 1985, ApJS, 57, 595

Coulson, I.M., & Caldwell, J.A.R. 1985, SAAO Circulars, 9, 5

Freedman, W.L., Grieve, G.R., & Madore, B.F. 1985, ApJS, 59, 311

Freedman, W.L. 1988, ApJ, 326, 691

Gibson B.K et al. 2000, ApJ, 529, 723

Gieren, W. 1981, ApJS, 47, 315

Gieren, W., Geisler, D., Richtler, T., Pietrzyński, G., Dirsch, B. 2001, The Messenger, 106, 15

Kiss, L.L. 1998, MNRAS, 297, 825

Labhardt, L., Sandage, A., & Tammann, G.A. 1997, *A&A*, 322, 751

Laney, C.D., & Stobie, R.S., 1992, *A&AS*, 93, 93

Madore, B.F. 1975, *ApJS*, 29, 219

Martin, W.L., & Warren, P.R. 1979, *South African Astron. Obs. Circ.*, No. 4, 98

Moffett, T.J., & Barnes, T.G. 1984, *ApJS*, 55, 389

Moffett, T.J., Gieren, W.P., Barnes, T.G., & Gomez, M. 1998, *ApJS*, 117, 135

Ngeow, C., Kanbur, S. M., Nikolaev, S., Tanvir, N., & Hendry, M. 2003, *ApJ*, 586, 959

Nikolaev, S., Drake, A.J., Keller, S.C., Cook, K.H., Dalal, N., Griest, K., Welch, D.L., & Kanbur, S. M. 2004, *ApJ*, 601, 260

Paczyński, B., & Pindor, B. 2000, *ApJ*, 533, L103

Persson, S.E., Madore, B.F., Krzeminski, W., Freedman, W.L., Roth, M., & Murphy, D.C. 2004, *AJ*, 128, 2239

Pojmański, G., 2002, *Acta Astron.*, 52, 397

Sebo, K.M., Rawson, D., Mould, J., Madore, B.F., Putman, M.E., Graham, J.A., Freedman, W.L., Gibson, B.K., & Germany, L.M. 2002, *ApJS*, 142, 71

Stetson P.B. 1996, *PASP*, 108, 851

Udalski, A., Soszyński, I., Szymański, M., Kubiak, M., Pietrzyński, G., Woźniak, P., & Źebruń, K. 1999, *Acta Astron.*, 49, 223

Welch, D.L., Wieland, F., McAlary, C.W., McGonegal, R., Madore, B.F., McLaren, R.A., & Neugebauer, G. 1984, *ApJS*, 54, 547

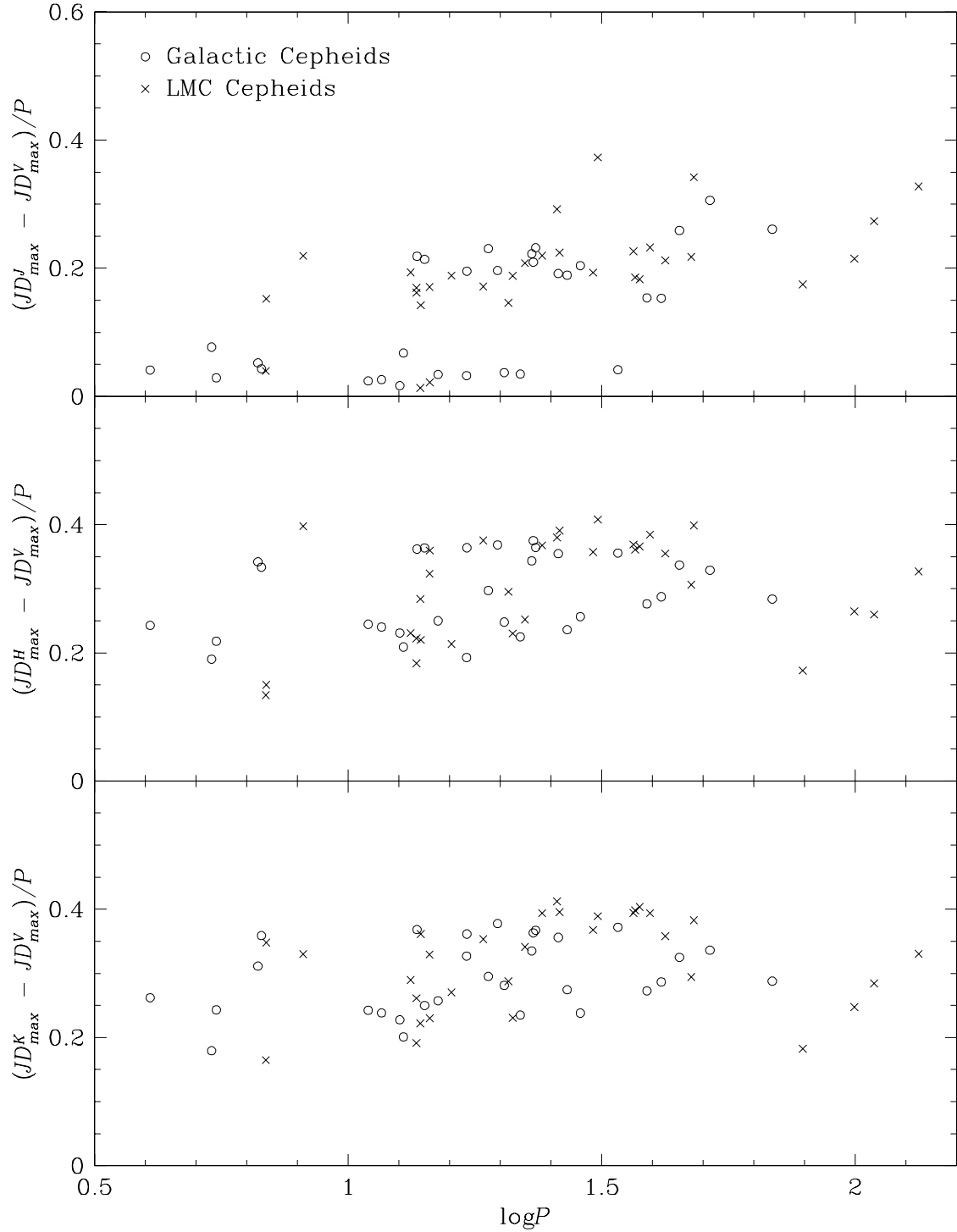


Fig. 1.— Phase lags between NIR and V -band light curves versus logarithm of the period. Circles indicate Galactic Cepheids, crosses – LMC Cepheids.

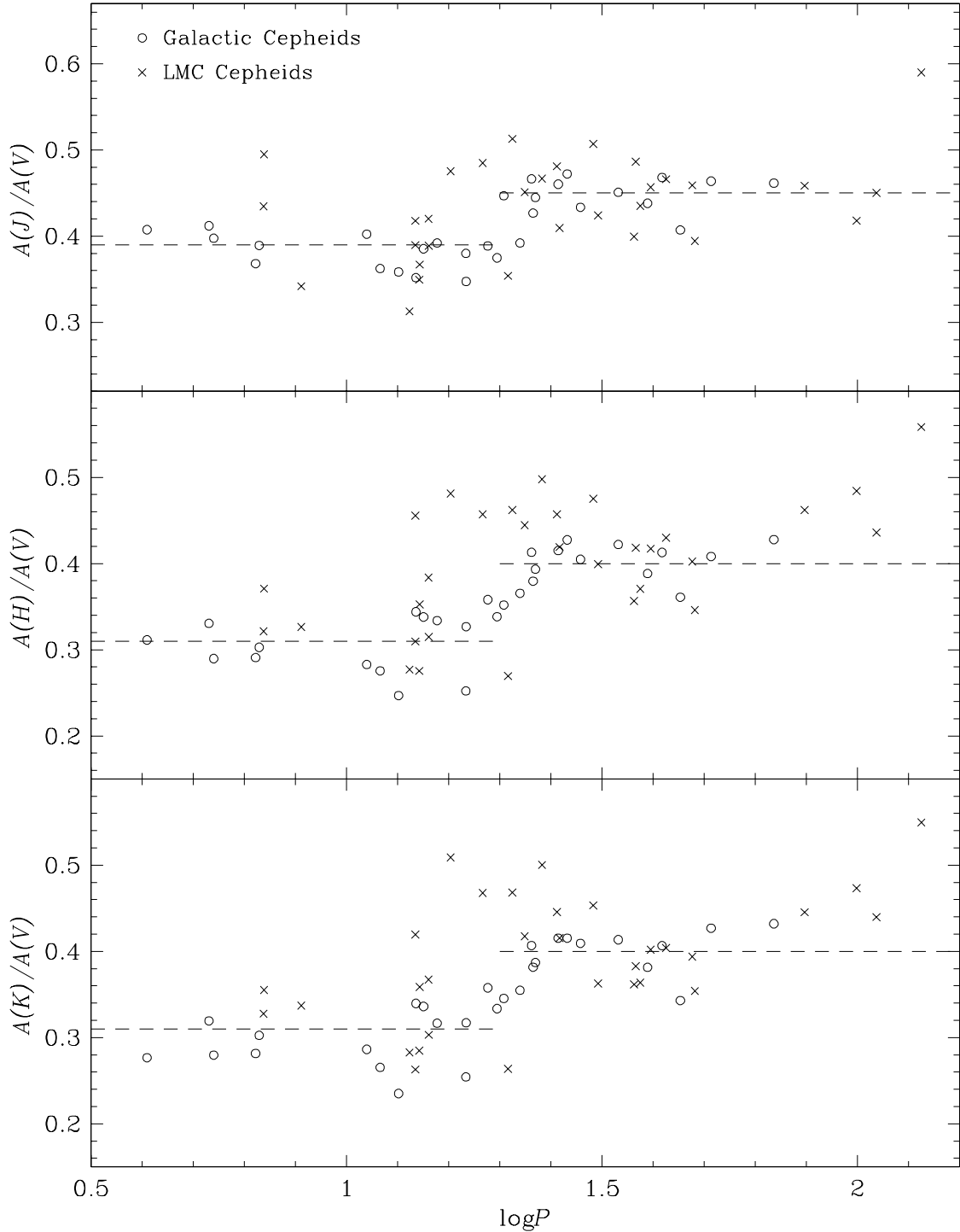


Fig. 2.— Amplitude ratios of NIR and V -band light curves versus the logarithm of the periods. Circles indicate Galactic Cepheids, crosses – LMC Cepheids. Dashed lines mark adopted mean values of the amplitude ratios for shorter and longer-period Cepheids.

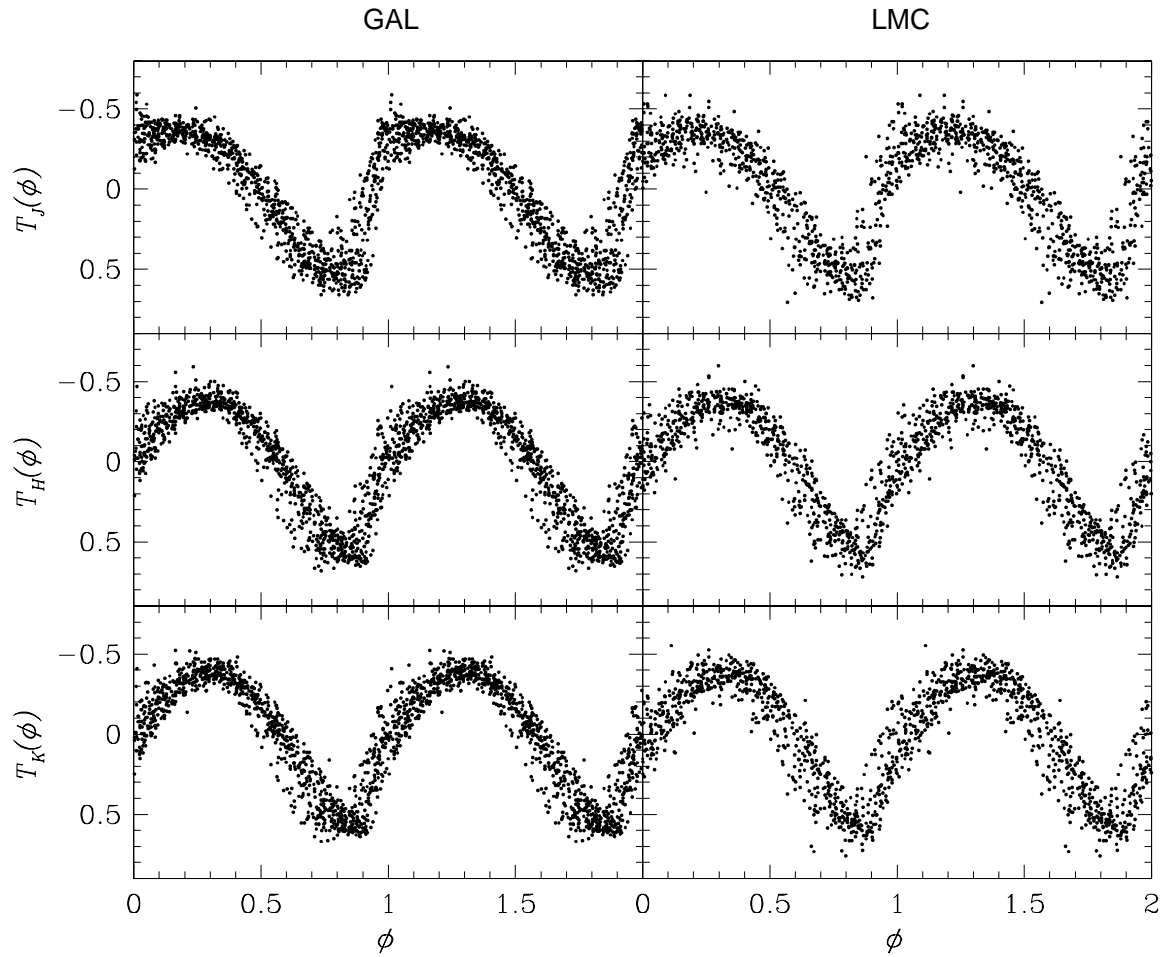


Fig. 3.— Template J , H , and K light curves for fundamental-mode Cepheids from the Galaxy and LMC.

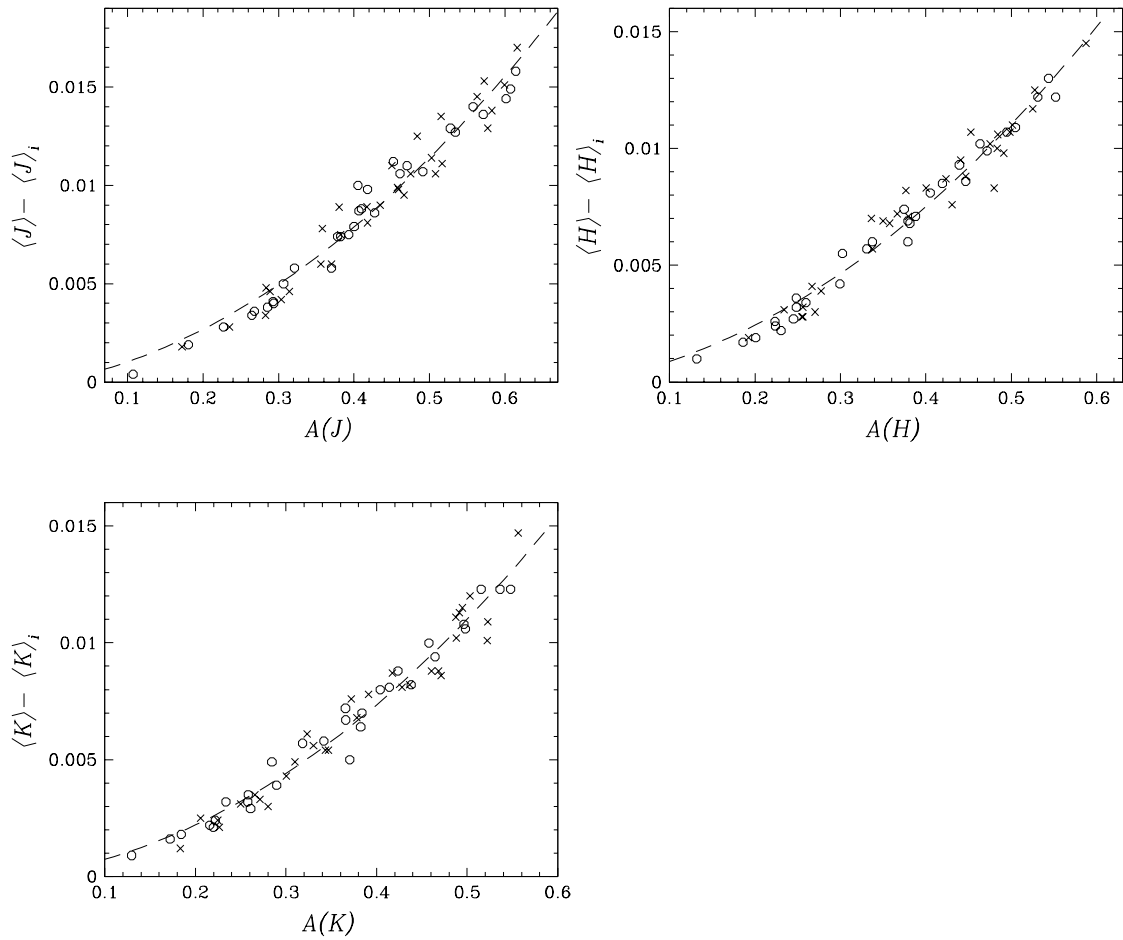


Fig. 4.— Differences between magnitude-averaged and intensity-averaged mean magnitudes versus amplitudes in J , H , and K bands. Circles indicate Galactic Cepheids, crosses – LMC Cepheids. Dashed lines are least-squares fits to a quadratic function.

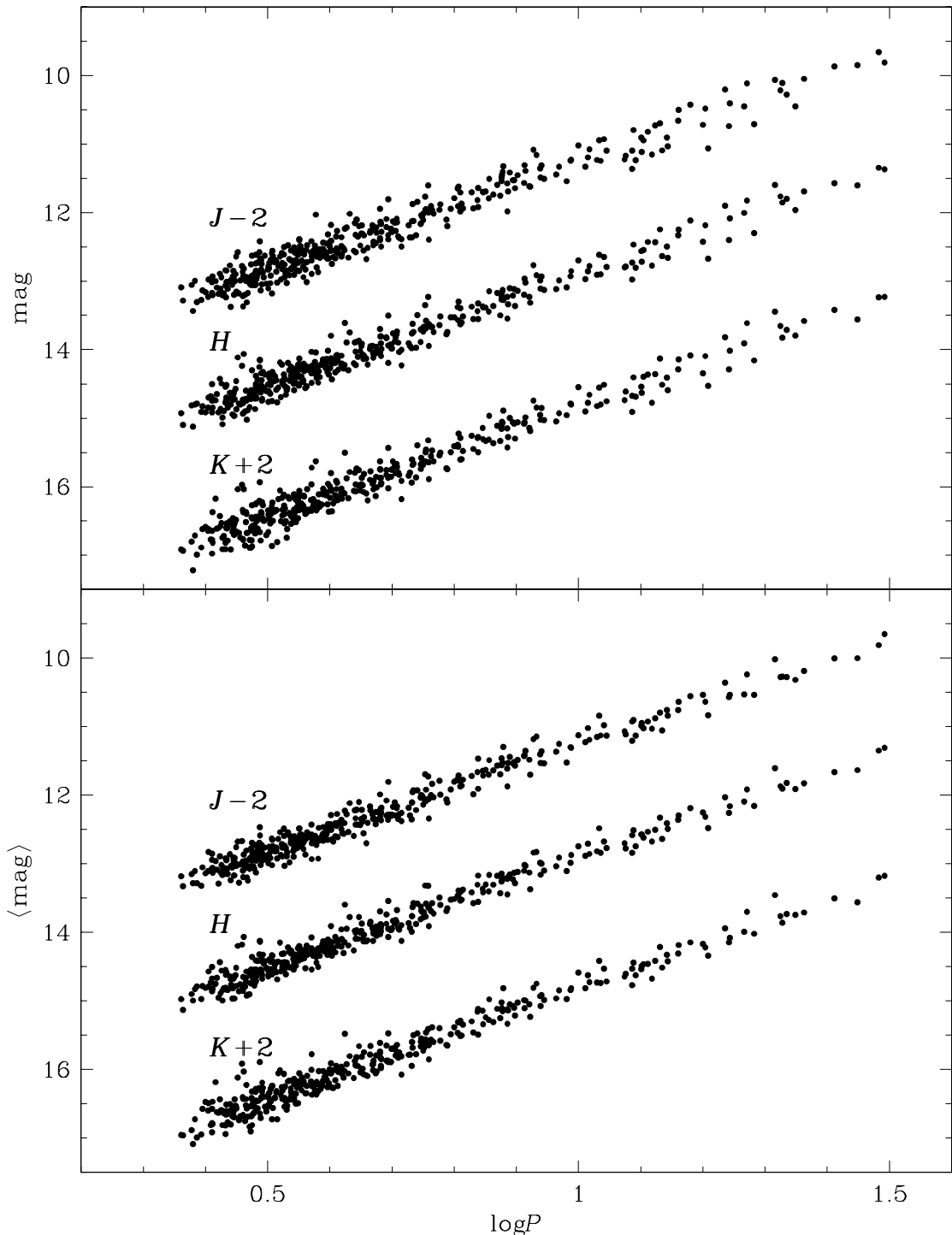


Fig. 5.— Near-infrared period–luminosity diagrams for fundamental-mode Cepheids in the LMC. *Top*: Single-epoch random-phase 2MASS photometry; *bottom*: mean magnitudes of the same stars derived by using OGLE-II I -band light curves, together with the algorithm described in this paper.

Table 1. List of Fundamental-Mode Cepheids Used in the Analysis.

Cepheid	Period [days]	$A(V)$ [mag]	$A(J)$ [mag]	$A(H)$ [mag]	$A(K)$ [mag]	Source of photometry
Galactic Cepheids						
BB Sgr	6.63712	0.610	0.225	0.178	0.172	c,d,l
BF Oph	4.06767	0.652	0.266	0.203	0.180	c,d,l,m
BN Pup	13.67253	1.217	0.428	0.419	0.413	a,g,l,n
CV Mon	5.37867	0.679	0.280	0.225	0.217	d,l
GY Sge	51.71139	0.593	0.275	0.242	0.253	l,n
KN Cen	34.02935	1.047	0.472	0.442	0.433	g,l,m,n,o
KQ Sco	28.69714	0.916	0.397	0.371	0.375	g,m,n,o
LS Pup	14.14729	0.994	0.383	0.336	0.334	g,l,n
RS Pup	41.44858	1.122	0.525	0.463	0.456	a,d,l
RU Sct	19.70259	1.107	0.415	0.374	0.369	d,l
RY Sco	20.32186	0.840	0.375	0.296	0.290	a,d,g,m,o
SU Cru	12.84922	0.608	0.107	0.057	0.051	a,g,n
S Vul	68.62792	0.578	0.267	0.247	0.250	l
SV Vul	45.00545	1.049	0.427	0.379	0.360	d,l,h,j
SW Vel	23.42489	1.310	0.583	0.516	0.507	g,l,m,n,o
SZ Aql	17.14049	1.201	0.417	0.393	0.381	d,l,h,n
T Mon	27.03014	1.010	0.477	0.432	0.420	d,g,l,m,o
U Car	38.82372	1.186	0.520	0.461	0.453	a,g,l,m,o
U Nor	12.64452	0.996	0.357	0.246	0.234	a,g,n
U Sgr	6.74535	0.735	0.286	0.223	0.222	c,d,l
UU Mus	11.63620	1.074	0.389	0.296	0.285	a,g
V Cen	5.49397	0.782	0.311	0.227	0.219	c,l,m,o
VW Cen	15.03728	0.999	0.392	0.334	0.317	g,m,n,o
VY Car	18.90336	1.042	0.405	0.373	0.373	a,g,m,o
VZ Pup	23.17559	1.297	0.554	0.492	0.495	a,g,l,m,n,o
WZ Car	23.01515	1.312	0.612	0.542	0.534	a,g,l,m,n,o
WZ Sgr	21.85096	1.127	0.442	0.412	0.400	a,d,g,l,n
X Pup	25.96654	1.318	0.607	0.547	0.548	a,d,l,m,n,o
XX Cen	10.95328	0.907	0.363	0.255	0.258	a,e,m,o
Y Oph	17.12588	0.494	0.188	0.125	0.126	d,g,l

Table 1—Continued

Cepheid	Period [days]	$A(V)$ [mag]	$A(J)$ [mag]	$A(H)$ [mag]	$A(K)$ [mag]	Source of photometry
LMC Cepheids						
HV879	36.82828	1.182	0.575	0.494	0.453	b,i
HV883	133.35058	1.172	0.692	0.655	0.644	a,b,f,i,p
HV885	20.70351	0.909	0.322	0.245	0.240	k
HV887	14.48897	1.088	0.423	0.343	0.330	k
HV889	25.80413	0.929	0.447	0.424	0.414	a,k
HV892	15.98925	1.014	0.482	0.488	0.516	k
HV893	21.11783	0.997	0.511	0.461	0.467	k
HV899	31.05049	1.299	0.551	0.519	0.471	a,b,i,k
HV900	47.50348	1.006	0.462	0.405	0.396	a,b,i
HV901	18.46964	0.935	0.453	0.427	0.437	k
HV904	30.39899	1.204	0.610	0.572	0.546	k
HV909	37.56872	1.166	0.507	0.432	0.424	a,b,i
HV911	13.90935	1.079	0.396	0.381	0.387	k
HV914	6.87847	0.797	0.346	0.256	0.261	k
HV932	13.28336	1.216	0.380	0.337	0.344	k
HV953	48.05070	1.050	0.414	0.363	0.372	a,b,f
HV1013	24.13171	0.886	0.414	0.441	0.443	b
HV2257	39.38681	1.217	0.556	0.508	0.489	a,b,i
HV2270	13.62556	0.831	0.347	0.379	0.349	k
HV2279	6.89384	0.897	0.444	0.333	0.318	k
HV2291	22.31693	1.031	0.465	0.458	0.430	k
HV2294	36.54844	1.351	0.539	0.482	0.488	a,b,f
HV2324	14.46634	0.900	0.378	0.345	0.330	b,k
HV2338	42.19749	1.207	0.563	0.519	0.488	a,b,i
HV2339	13.87914	0.974	0.340	0.268	0.277	k
HV2352	13.63052	0.752	0.293	0.233	0.198	b,p
HV2827	78.82556	0.585	0.268	0.270	0.261	b,i
HV2883	108.94612	1.473	0.663	0.642	0.648	a,b,f,i
HV5497	99.58612	0.524	0.219	0.254	0.248	a,b,f,i,p
HV12700	8.15255	0.531	0.181	0.173	0.179	b
HV12815	26.11563	1.155	0.473	0.484	0.480	b,i

Table 1—Continued

Cepheid	Period	$A(V)$	$A(J)$	$A(H)$	$A(K)$	Source of photometry
	[days]	[mag]	[mag]	[mag]	[mag]	

References. — a – Madore (1975); b – Martin & Warren (1979); c – Gieren (1981); d – Moffett & Barnes (1984); e – Coulson, Caldwell & Gieren (1985); f – Freedman, Grieve & Madore (1985); g – Coulson & Caldwell (1985); h – Barnes et al. (1997); i – Moffett et al. (1998); j – Kiss (1998); k – Udalski et al. (1999); l – Berdnikov, Dambis & Vozyakova (2000, and references therein); m – Berdnikov & Turner (2001); n – Pojmański (2002); o – Bersier (2002); p – Sebo et al. (2002).

Table 2. Adopted Amplitude Ratios of the NIR and Visual Light Curves of Cepheids.

Period	$A(J)/A(V)$	$A(H)/A(V)$	$A(K)/A(V)$	$A(J)/A(I)$	$A(H)/A(I)$	$A(K)/A(I)$
$\log P < 1.3^a$	0.39	0.32	0.31	0.63	0.50	0.49
$\log P \geq 1.3^a$	0.45	0.40	0.40	0.70	0.63	0.62

^aIn the LMC we adopted $\log P = 1.1$ to separate Cepheids with smaller and larger amplitude ratios.

Table 3. Fourier Coefficients of the Template Light Curves.

	$T_J^V(\phi)$	$T_H^V(\phi)$	$T_K^V(\phi)$	$T_J^I(\phi)$	$T_H^I(\phi)$	$T_K^I(\phi)$
A_1	0.432	0.438	0.440	0.432	0.433	0.434
A_2	0.109	0.089	0.082	0.110	0.094	0.085
A_3	0.058	0.039	0.035	0.060	0.046	0.043
A_4	0.039	0.019	0.021	0.038	0.023	0.020
A_5	0.025	0.019	0.012	0.029	0.022	0.016
A_6	0.016	0.018	0.013	0.015	0.021	0.015
A_7	0.010	0.011	0.010	0.010	0.016	0.013
ϕ_1	1.734	1.262	1.201	1.863	1.397	1.333
ϕ_2	2.747	2.303	2.174	2.901	2.543	2.419
ϕ_3	3.079	2.913	2.757	3.324	3.266	3.097
ϕ_4	3.671	3.394	3.448	3.934	3.886	3.794
ϕ_5	4.253	3.318	3.406	4.678	3.813	3.765
ϕ_6	4.460	3.972	3.658	5.164	4.380	4.475
ϕ_7	5.429	4.727	4.719	5.851	5.245	5.149

Table 4. Errors of the Estimated Mean Magnitudes.

Cepheid	Galactic Cepheids			LMC Cepheids			
	$\sigma_{\langle J \rangle}$	$\sigma_{\langle H \rangle}$	$\sigma_{\langle K \rangle}$	Cepheid	$\sigma_{\langle J \rangle}$	$\sigma_{\langle H \rangle}$	$\sigma_{\langle K \rangle}$
BB Sgr	0.030	0.025	0.026	HV879	0.055	0.029	0.034
BF Oph	0.027	0.021	0.019	HV883	0.113	0.097	0.107
BN Pup	0.042	0.026	0.027	HV885	0.039	0.050	0.047
CV Mon	0.025	0.023	0.020	HV887	0.049	0.043	0.042
GY Sge	0.024	0.022	0.022	HV889	0.055	0.050	0.052
KN Cen	0.034	0.025	0.024	HV892	0.083	0.073	0.076
KQ Sco	0.017	0.021	0.029	HV893	0.050	0.034	0.037
LS Pup	0.033	0.025	0.025	HV899	0.084	0.066	0.060
RS Pup	0.042	0.029	0.027	HV900	0.058	0.042	0.048
RU Sct	0.027	0.023	0.026	HV901	0.046	0.051	0.058
RY Sco	0.018	0.019	0.020	HV904	0.079	0.055	0.051
S Cru	0.046	0.040	0.041	HV909	0.070	0.061	0.063
S Vul	0.034	0.030	0.026	HV911	0.036	0.028	0.035
SV Vul	0.043	0.045	0.039	HV914	0.041	0.037	0.041
SW Vel	0.089	0.060	0.056	HV932	0.044	0.026	0.029
SZ Aql	0.031	0.016	0.017	HV953	0.072	0.056	0.060
T Mon	0.025	0.021	0.018	HV1013	0.051	0.044	0.050
U Car	0.048	0.034	0.034	HV2257	0.052	0.034	0.032
U Nor	0.068	0.057	0.056	HV2270	0.037	0.046	0.045
U Sgr	0.024	0.021	0.018	HV2279	0.060	0.046	0.038
UU Mus	0.047	0.040	0.041	HV2291	0.037	0.032	0.027
V Cen	0.035	0.030	0.029	HV2294	0.060	0.046	0.044
VW Cen	0.033	0.024	0.024	HV2324	0.034	0.033	0.033
VY Car	0.053	0.039	0.039	HV2338	0.067	0.048	0.053
VZ Pup	0.059	0.044	0.043	HV2339	0.068	0.051	0.051
WZ Car	0.087	0.056	0.051	HV2352	0.056	0.037	0.034
WZ Sgr	0.019	0.017	0.019	HV2827	0.039	0.041	0.041
X Pup	0.070	0.043	0.040	HV2883	0.094	0.079	0.083
XX Cen	0.082	0.067	0.065	HV5497	0.056	0.059	0.059
Y Oph	0.036	0.029	0.027	HV12700	0.031	0.025	0.036
				HV12815	0.077	0.057	0.065

